Supporting Information

A general strategy for enhancing photoluminescence of TMD quantum sheets

Zhangqiang Li[a,b#], *Xuanping Zhou*[a,b#], *Ce Zhao*[a,b], *Liuyang Xiao*[a,b], *Yong Zhang*[*a,b]

[a] CAS Key Laboratory of Nanosystem and Hierarchical Fabrication, CAS Center for Excellence in Nanoscience, National Center for Nanoscience and Technology, Beijing 100190, P. R. China.

[b] University of Chinese Academy of Sciences, Beijing 100049, P. R. China.

[#] These authors contributed equally to this work

Corresponding Author

* E-mail: zhangyong@nanoctr.cn

Experimental Section

***Material*:** All chemicals and analytical reagents were utilized in their original form without additional purification. Tungsten disulfide (powder, 99.99%), molybdenum diselenide (powder, 99.99%), tungsten diselenide (powder, 99.99%), and bismuth selenide (powder, 99.99%) were purchased from Aladdin Bio-Chem Technology Co., Ltd. Potassium bromide (SP, 99.5%) was purchased from Tianjin Tianguang Optics Instrument Co., Ltd. Tetrahydrofuran (THF) (SP, 99.5%), N-methyl-2-pyrrolidone (NMP) (AR), aqueous ammonia (25%-28%), dichloroethane (AR), tetraethyl orthosilicate (AR), and poly(methyl methacrylate) (PMMA) (Transmittance > 92%) were purchased from Shanghai Macklin Biochemical Co., Ltd. Isopropanol (AR) and n-hexane (AR) were purchased from Tianjin Damao Chemical Reagent Factory. Porous anodic alumina (PAA) (0.02 μm pore size) was purchased from Whatman. The commercial InGaN chips and thermal-curable silicone resin were purchased from Sanan Optoelectronics Co., Ltd.

***Synthesis of intrinsic quantum sheets (I-QSs)*:** The I-QSs were prepared by a combination of silica-assisted ball-milling and sonication-assisted solvent exfoliation.[1] Initially, 200 mL of ethanol was heated to 70℃ and stirred, then 40 mL of tetraethyl orthosilicate was added. The mixture was stirred and heated for 20 minutes. Next, 40 mL of ammonia and 40 mL of water were added, with heating and stirring for 2 hours. The mixture was centrifuged, washed with ethanol, and vacuum-dried to produce 450 nm silica microspheres. A mixture of TMD powders (0.7 g), silica microspheres (7 g), and agate balls (70 g) were ball-milled at 500 rpm for 12 hours. After ball-milling, the agate balls were removed. The mixture was dispersed in NMP with a concentration of approximately 55 mg/mL for sonication (Vibra-Cell Ultrasonic Liquid Processor, VCX800, SONICS) at 240 W for 5 hours. The TMD QSs filtrate were collected through centrifugation and PAA membrane with a 0.02 μm pore size. The TMD QSs powders were obtained by preparing a precipitation system with a volume ratio of 5/10/2 (QSs filtrate/n-hexane/IPA) and centrifuged at 8000 rpm for 30 minutes, followed by vacuum drying.

Synthesis of passivation quantum sheets (P-QSs): P-QSs were prepared by redispersing the I-QSs powder in THF (concentration of 0.04 mg/mL), and then heated in silicone oil at 100℃ for 4 hours at a constant temperature. The TMD QSs

were washed with dichloroethane 2 times after heating, then vacuum drying (50℃, 2 hours). Subsequently, 1 mL of NMP dispersant was added to redisperse the QSs. Ultrasonic treatment at 100 W for 10 minutes (using a 200 W ultrasonic cleaning machine) was performed to obtain passivated QSs dispersion. All the QSs-PMMA thin films described in this study were fabricated in the following procedure: 400 mg PMMA were dissolved in 1 mL NMP and stirred at 50℃ for 12 hours to prepare a 400 mg/mL polymer solution. Then, the passivated QSs dispersion and polymer solution were mixed by stirring at a loading amount of 0.1 wt% QSs (QSs/PMMA=1/1000). Finally, the solution was transferred to PTFE mold (0.4 ml in total capacity) and kept at 40℃ for 24 hours.

***Fabrication of Light Emitting Diodes (LEDs)*:** The white LEDs were fabricated by coating P-WS_2 QSs on the commercial 382 nm InGaN chips. The passivated QSs (5 μL, 0.06 mg/mL in NMP) were coated on the InGaN LED chip and dried at 40℃ for 12 hours. Subsequently, the thermal-curable silicone resin (15 μL) was coated on the surface of the QSs layer, followed by thermal curing at 40℃ for 10 hours to obtain the solid-state white LEDs.

***Characterization*:** The transmission electron microscopy (TEM) and high-resolution TEM (HRTEM) images were collected using the FEI Tecnai F20 U-TWIN microscope operating at an acceleration voltage of 200 kV. The atomic force microscope (AFM) images were performed utilizing the Bruker MultiMode 8 AFM. The X-ray diffraction (XRD) measurements were carried out on a D/Max-TTRIII (CBO) with Cu Kα radiation (λ = 1.54056 Å). Fourier-transform infrared (FTIR) spectra were recorded on a PerkinElmer Spotlight 200i by potassium bromide tablet. X‐ray photoelectron spectroscopy (XPS) analyses were performed utilizing an EscaLab 250Xi electron spectrometer from ThermoFisher Scientific, employing 300 W Al Kα radiation. The ultraviolet-visible (UV-vis) absorption spectra were recorded using a Lambda 950 spectrophotometer from PerkinElmer. The photoluminescence (PL) and electroluminescence (EL) spectra were collected at room temperature on HORIBA FluoroMax Plus. A time-correlated single photon counting (TCSPC) method was employed to measure the PL lifetime using HORIBA FluoroMax Plus and TCSPC instrument. The instrument response function (IRF) was measured by

SiO_2. The photoluminescence quantum yield (PLQY) of TMD QSs were measured at room temperature by HORIBA FluoroMax Plus and integrating sphere attachment.

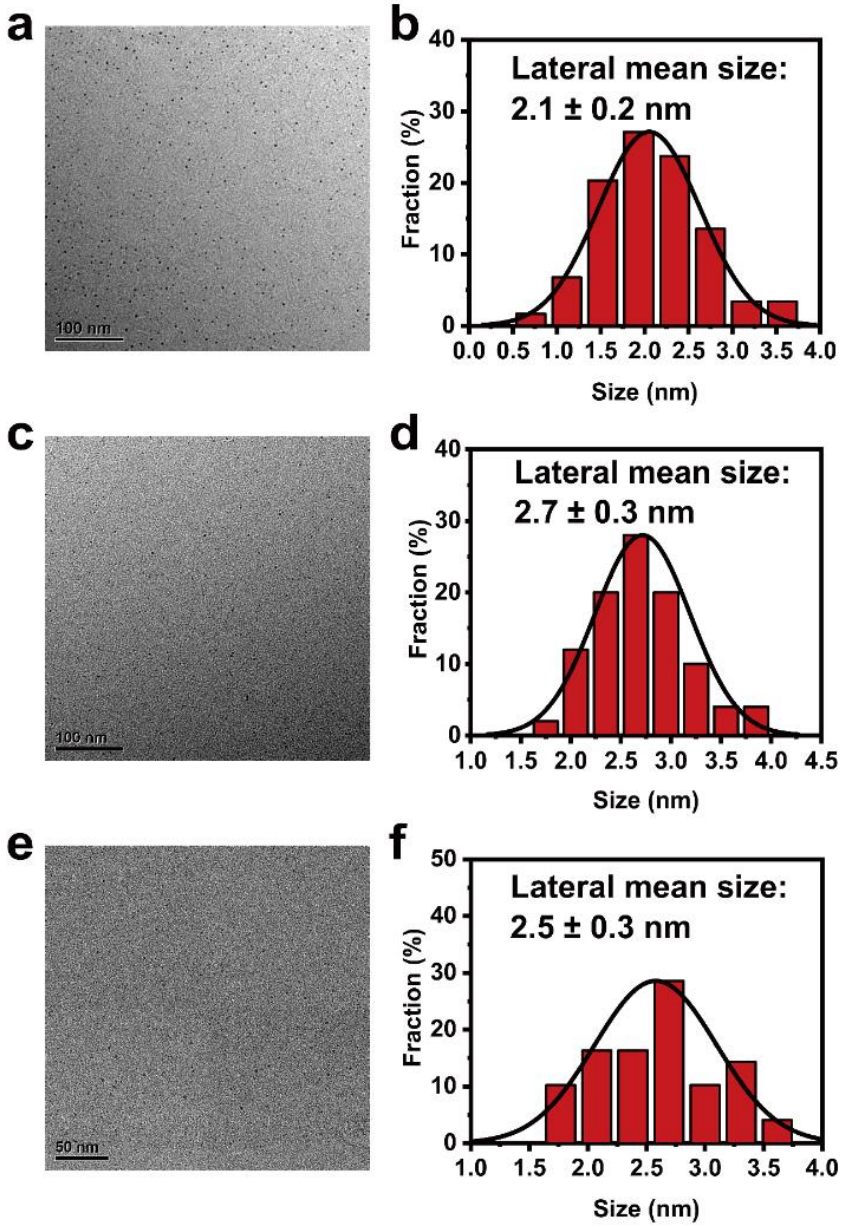

Figure S1. TEM-based measurement of the sizes of intrinsic QSs. (a) TEM image and (b) Size distribution of I-$MoSe_2$ QSs. (c) TEM image and (d) Size distribution of I-Bi_2Se_3 QSs. (e) TEM image and (f) Size distribution of I-WSe_2 QSs.

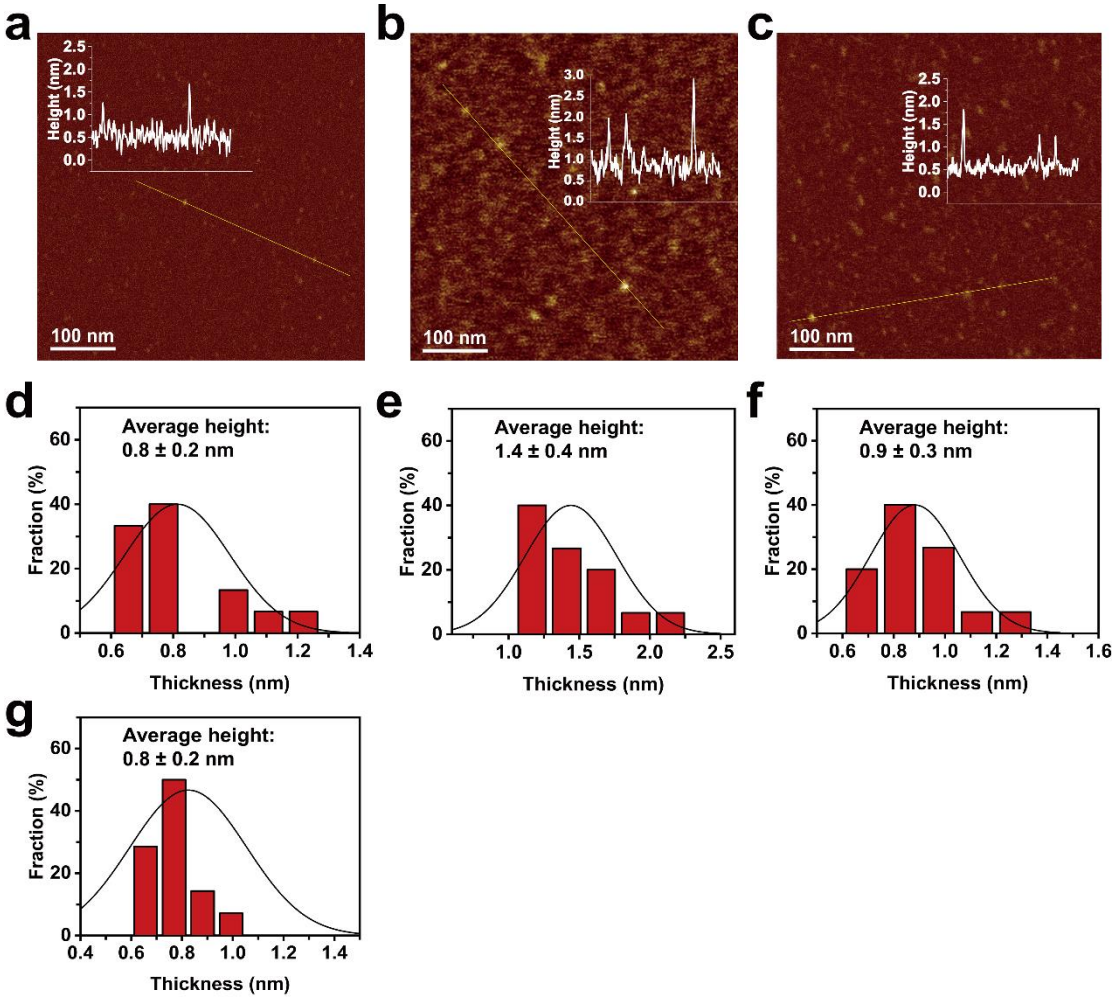

Figure S2. AFM images of (a) I-$MoSe_2$ QSs, (b) I-Bi_2Se_3 QSs, and (c) I-WSe_2 QSs. The average height of (d) I-$MoSe_2$ QSs, (e) I-Bi_2Se_3 QSs, (f) I-WSe_2, and (g) I-WS_2 QSs. The corresponding height profile along the line in the AFM images.

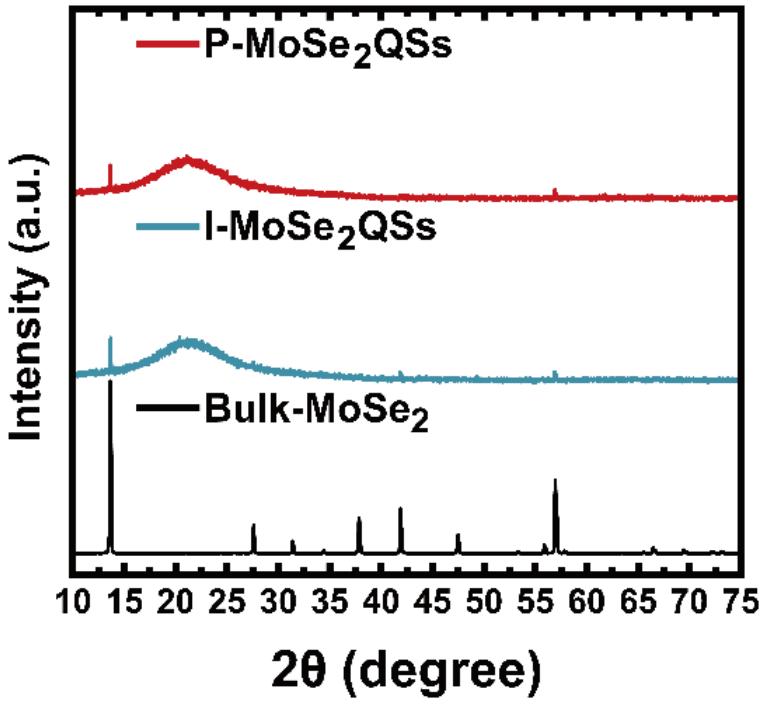

Figure S3. XRD patterns of $MoSe_2$.

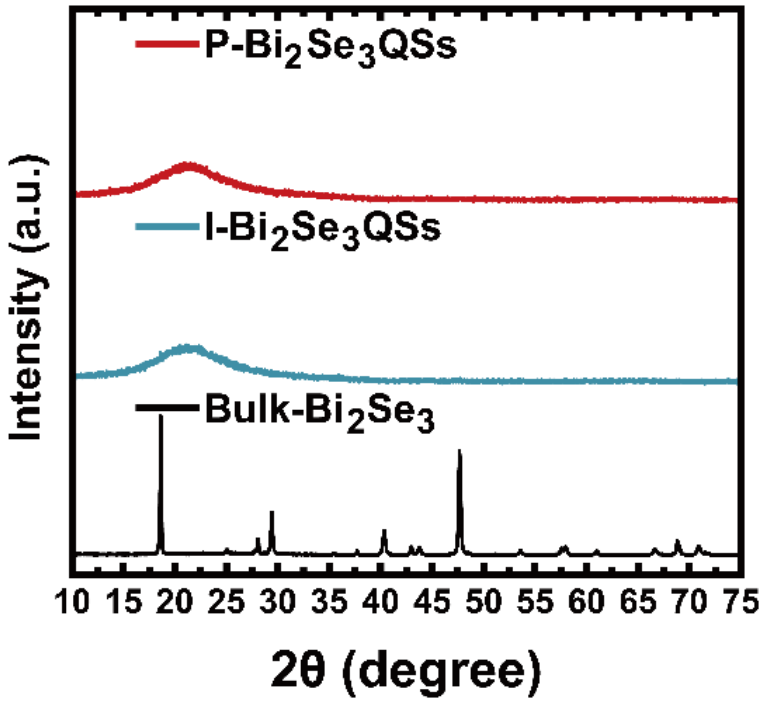

Figure S4. XRD patterns of Bi_2Se_3.

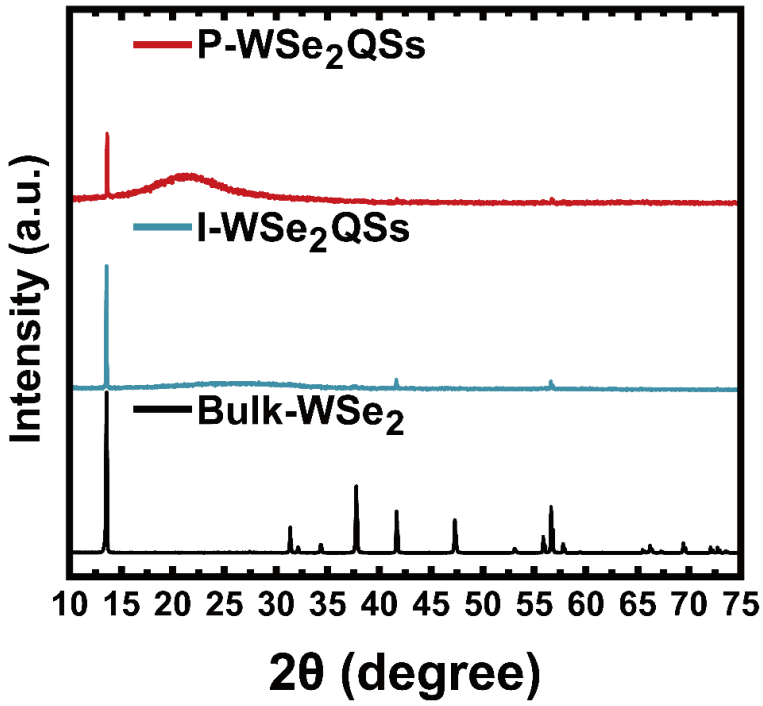

Figure S5. XRD patterns of WSe_2.

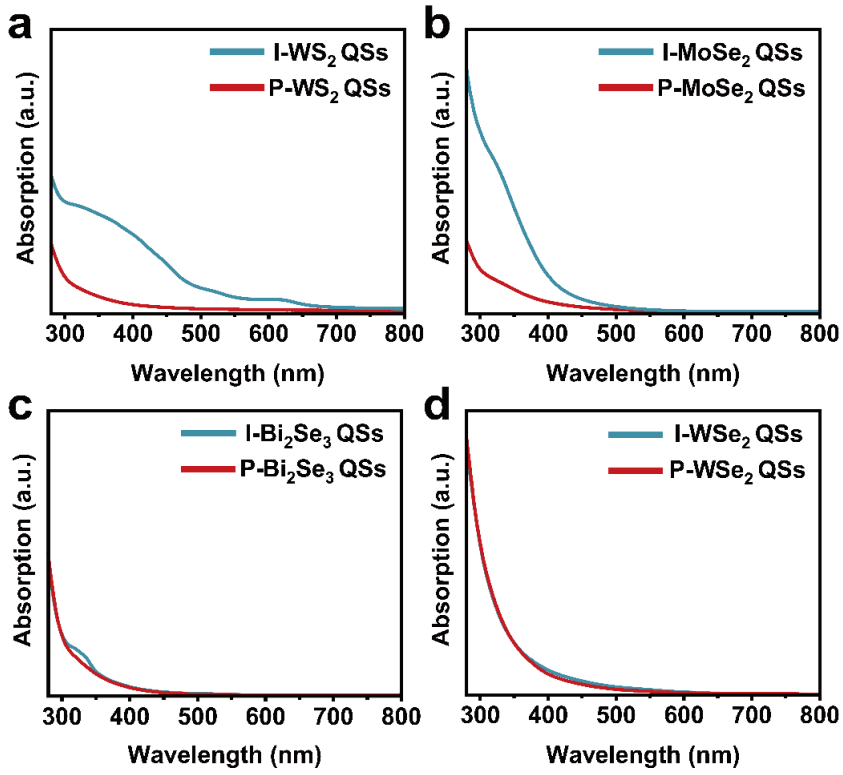

Figure S6. UV-vis absorption spectra of TMD QSs. (a) WS_2 QSs. (b) $MoSe_2$ QSs. (c) Bi_2Se_3 QSs. (d) WSe_2 QSs.

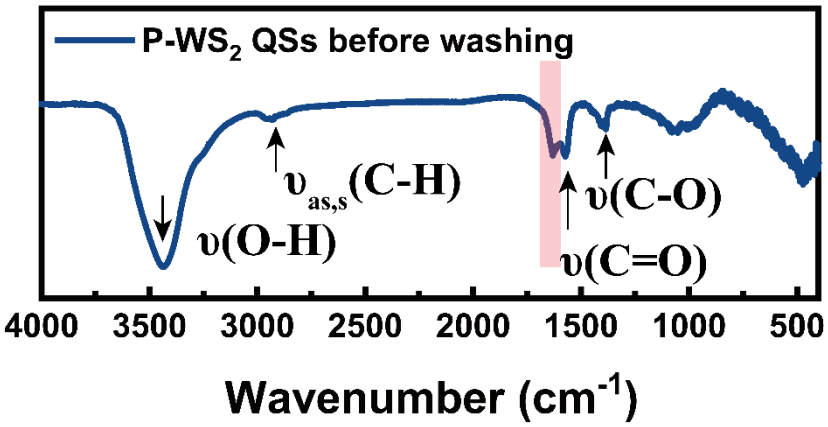

Figure S7. FTIR spectrum of WS_2 QSs before dichloroethane washing. ν_s: vibration modes for symmetric stretching. ν_{as}: vibration modes for asymmetric stretching. Red area: skeletal vibrations of aromatic ring.

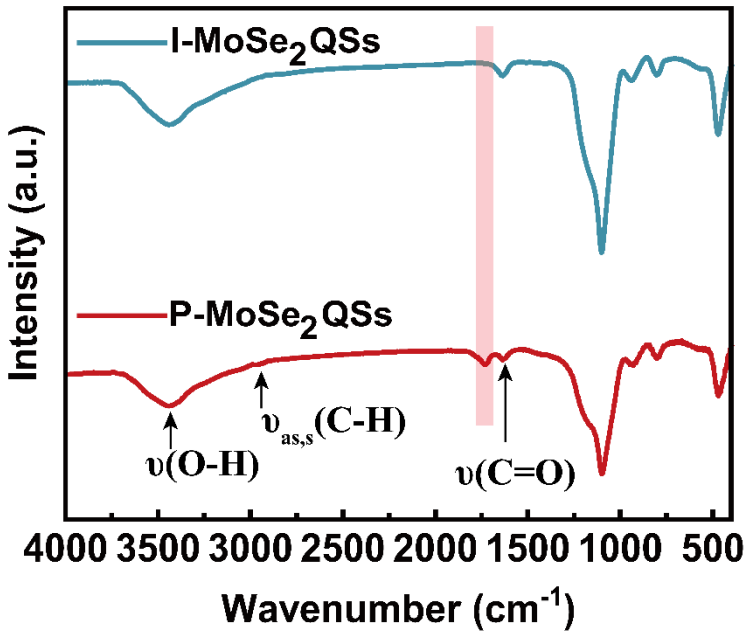

Figure S8. FTIR spectra of $MoSe_2$ QSs. ν_s: vibration modes for symmetric stretching. ν_{as}: vibration modes for asymmetric stretching. Red area: skeletal vibrations of aromatic ring.

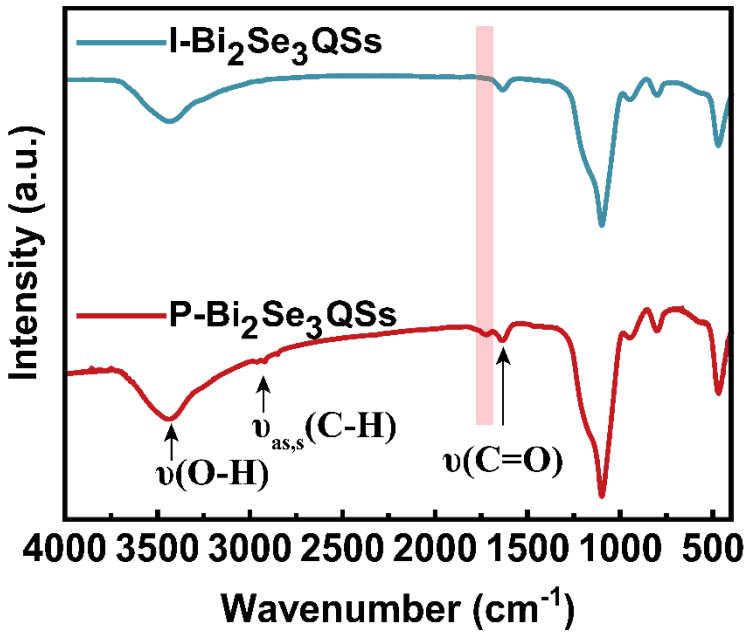

Figure S9. FTIR spectra of Bi_2Se_3 QSs. ν_s: vibration modes for symmetric stretching. ν_{as}: vibration modes for asymmetric stretching. Red area: skeletal vibrations of aromatic ring.

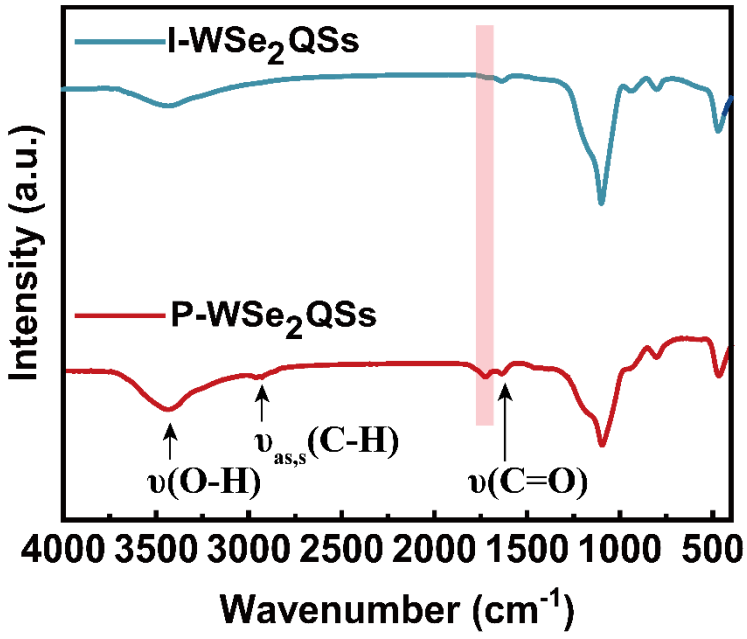

Figure S10. FTIR spectra of WSe_2 QSs. ν_s: vibration modes for symmetric stretching. ν_{as}: vibration modes for asymmetric stretching. Red area: skeletal vibrations of aromatic ring.

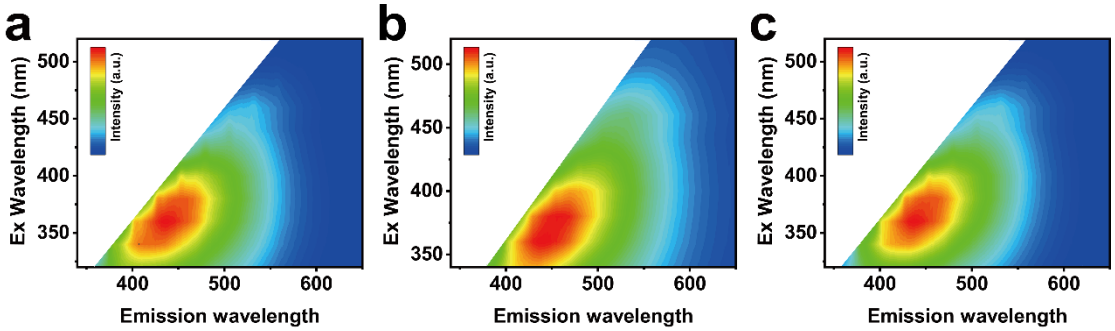

Figure S11. Excitation–emission matrices for P-QSs-PMMA. (a) P-$MoSe_2$ QSs-PMMA. (b) P-Bi_2Se_3 QSs-PMMA. (c) P-WSe_2 QSs-PMMA.

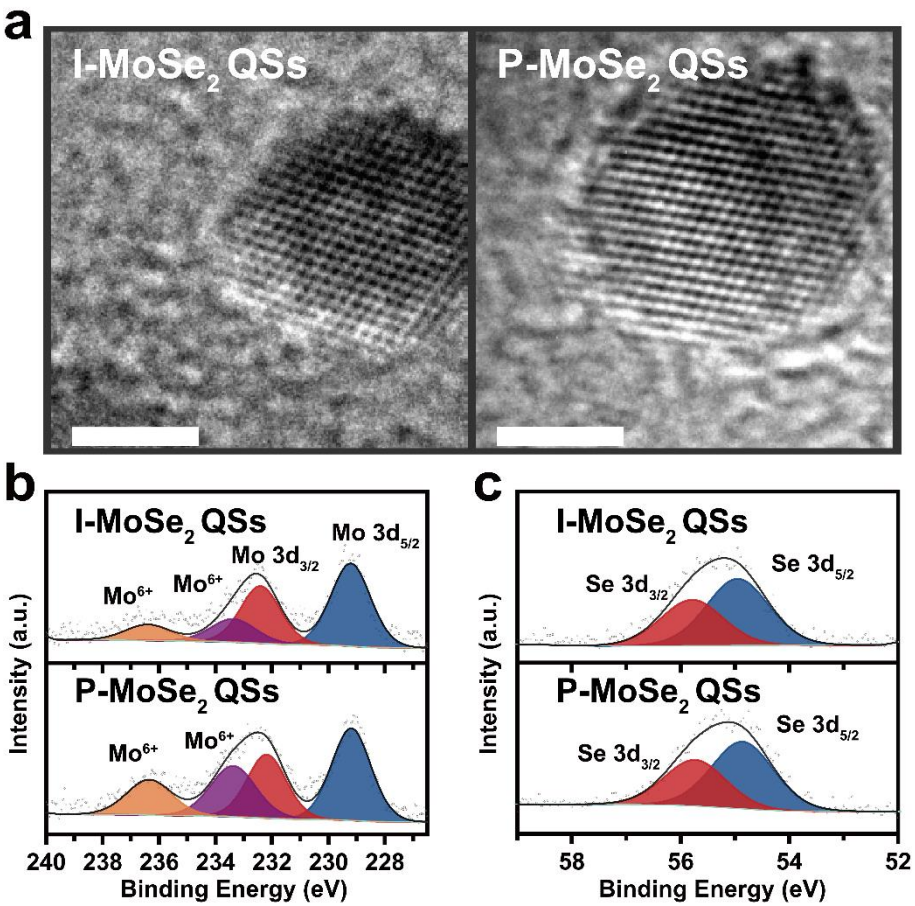

Figure S12. Structure elucidation of $MoSe_2$ QSs. (a) HRTEM images of $MoSe_2$ QSs. (b, c) XPS of $MoSe_2$ QSs. Scale bars in HRTEM are 2 nm.

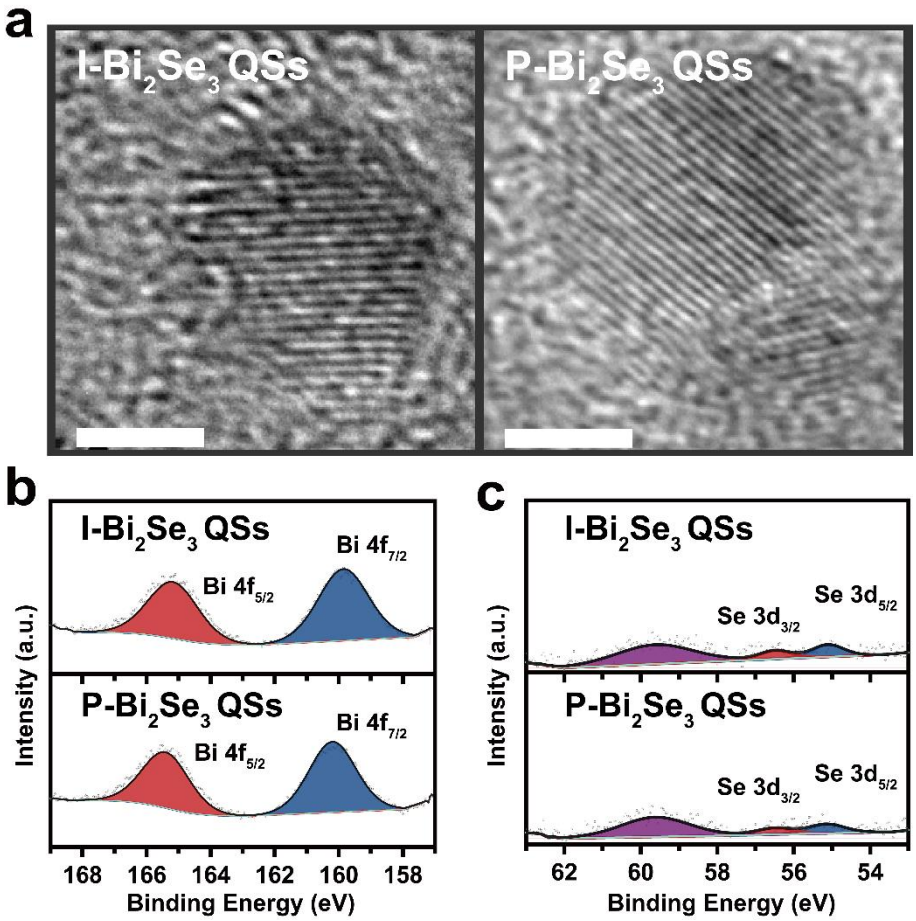

Figure S13. Structure elucidation of Bi_2Se_3 QSs. (a) HRTEM images of Bi_2Se_3 QSs. (b, c) XPS of Bi_2Se_3 QSs. Scale bars in HRTEM are 2 nm.

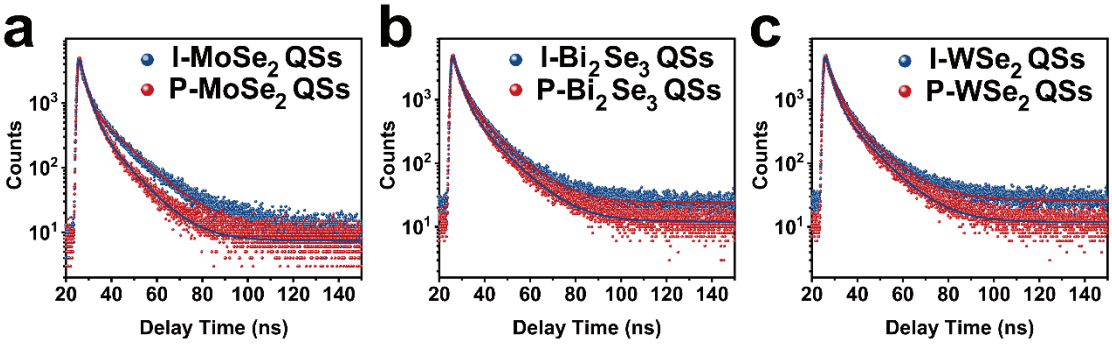

Figure S14. Lifetimes of TMD QSs. (a) $MoSe_2$ QSs. (b) Bi_2Se_3 QSs. (c) WSe_2 QSs.

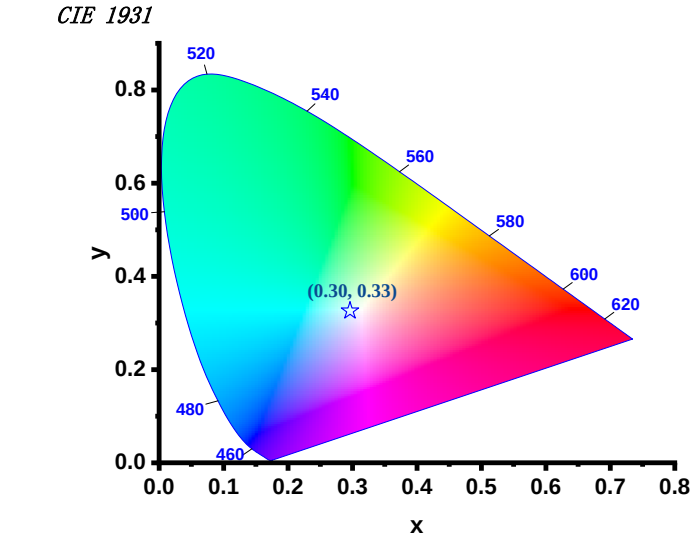

Figure S15. CIE value of P-WS_2 QSs LED.

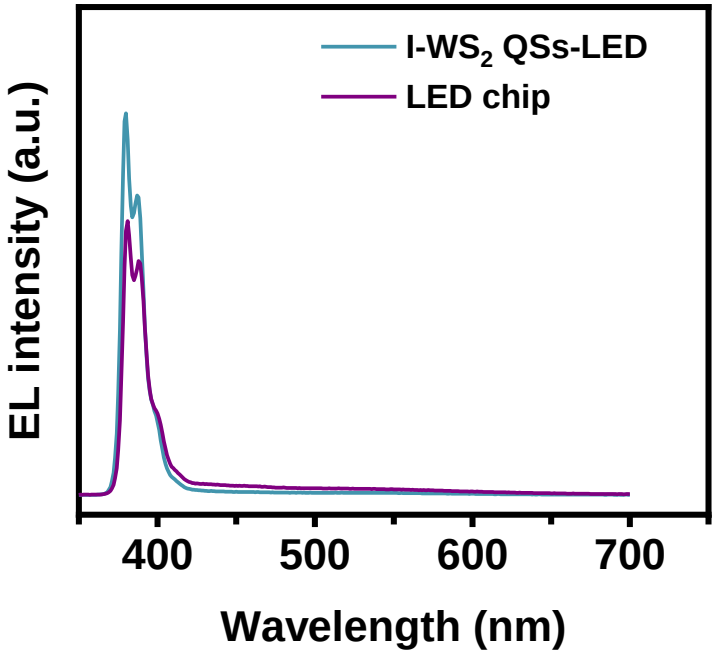

Figure S16. EL spectra of the LED chip and the I-WS_2 QSs-LED generated under a current of 10 mA.

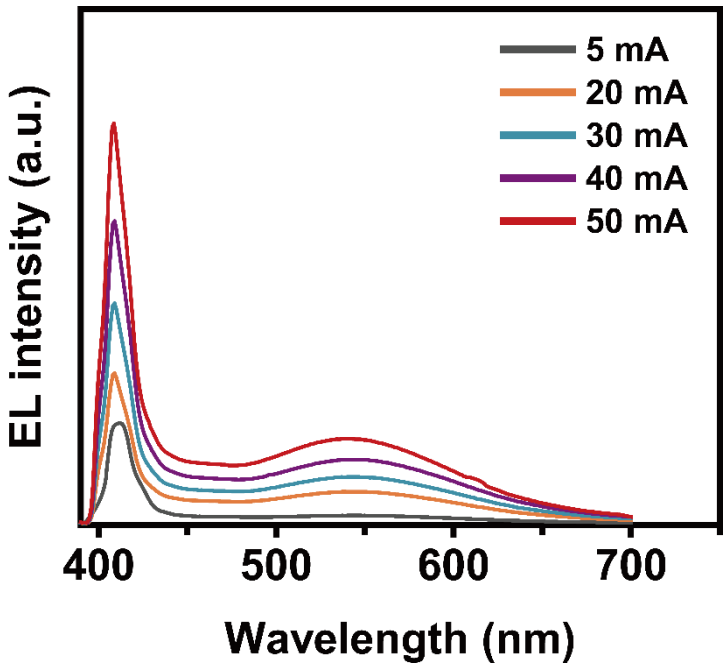

Figure S17. EL spectra of fabricated P-WS_2 QSs-LED at 5–50 mA operating currents.

Table S1. Atomic ratios obtained by partial-scan XPS spectra. X stands for W, Mo, Bi. Compared to I-QSs, the oxidation state X content of P-QSs is significantly increased. The binding energy of Bi^{4+} in P-Bi_2Se_3 is shifted towards higher binding energy.

X^{6+}/X^{4+}	WS_2	$MoSe_2$	Bi_2Se_3	WSe_2
I-QSs	0	0.32	-	0
P-QSs	1.41	0.57	-	1.89

Table S2. Multiexponential fitting for time-resolved PL spectra of TMD QSs-PMMA at emission wavelength of 467 nm when excited at 370 nm.

I-QSs	WS_2	$MoSe_2$	Bi_2Se_3	WSe_2
τ_1 (ns)	2.82(46.4%)	3.42(45.1%)	3.19(46.0%)	3.12(49.7%)
τ_2 (ns)	12.80(53.6%)	12.26(54.9%)	11.63(54.0%)	11.45(50.3%)
Average (ns)	8.18	8.27	7.75	7.31

Table S3. Multiexponential fitting for time-resolved PL spectral of TMD QSs-PMMA at emission wavelength of 467 nm when excited at 370 nm. Amongst, the PL dynamics have two distinct relaxation time scales, fast and slow decays, showing the fast decay of carrier recombination in the QSs became dominant.

P-QSs	WS_2	$MoSe_2$	Bi_2Se_3	WSe_2
τ_1 (ns)	2.32(77.3%)	2.78(64.5%)	2.94(55.3%)	2.86(55.6%)
τ_2 (ns)	8.08(22.7%)	10.55(35.5%)	11.43(44.7%)	11.27(44.4%)
Average (ns)	3.63	5.54	6.74	6.59

REFERENCES

1. Xu, Y.; Chen, S.; Dou, Z.; Ma, Y.; Mi, Y.; Du, W.; Liu, Y.; Zhang, J.; Chang, J.; Liang, C.; Zhou, J.; Guo, H.; Gao, P.; Liu, X.; Che, Y.; Zhang, Y., Robust Production of 2D Quantum Sheets from Bulk Layered Materials. *Mater. Horiz.* **2019,** *6* (7), 1416-1424.